Wind and Structures, Vol. 4, No. 2 (2001) 101-118
DOI: http://dx.doi.org/10.12989/was.2001.4.2.101

Pressure equalization of rainscreen facades: Analysis of the field data in the frequency domain

K. Suresh Kumar†

RWDI Inc., 650 Woodlawn Road West, Guelph, Ontario, N1K 1B8, Canada

J.A. Wisse‡

Faculty of Architecture, Building and Planning, FAGO, Technical University of Eindhoven (TUE), Postbus 513, 5600 MB Eindhoven, The Netherlands

Abstract. This paper reports the field measurements concerning pressure equalization of rainscreen facades carried out at the Technical University of Eindhoven (TUE) in the Netherlands. The field facility including the details of test panel, meteorological tower, instrumentation, data collection and analysis is presented. Results of investigations into cavity response for various leakage and venting configurations are discussed. Frequency domain techniques have been utilized to show the influence of wind as well as facade characteristics on the pressure equalization performance. Further, this paper presents an early attempt to synthesize the experimental results into existing building codes.

Key words: field measurements; pressure equalization; rainscreen facade.

1. Introduction

Pressure Equalized Rainscreen (PER) facades were introduced in the 1960's mainly to reduce rainwater penetration caused by wind-induced pressure differentials across the facade. Another advantage of PER facade is its ability to reduce wind loads acting on the rainscreen. A PER facade consists of two wall layers separated by a cavity. The wall layers facing the exterior and interior are respectively known as the rainscreen and the air barrier. The cavity is vented to the exterior by openings on the rainscreen that allows equalization of exterior pressure with cavity pressure. The state-of-the-art information concerning pressure equalized rainscreen approach to wall design has been documented (Anderson & Gill 1988, Suresh Kumar 1998a, Suresh Kumar 2000). Although the pressure equalized rainscreen concept is not new in the construction industry, little is known about the effect of parameters related to wind loading (mean pressures, temporal pressure variations, spatial pressure variations) and parameters related to facade characteristics (venting area, venting location and their distribution, leakage area, airflow characteristics of venting and leakage, cavity volume, stiffness of rainscreen and air barrier) on pressure equalization performance. For better design of PER facades, further research into the effects of various parameters is needed before objective standards

† Senior Engineer, Formerly, Post-doctoral Fellow at the Faculty of Architecture, Building and Planning, Technical University of Eindhoven, The Netherlands
‡ Professor

or codes for their design can be set. Therefore, an extensive investigation, consisting of full-scale monitoring and computer simulations, has been carried out at TUE (Suresh Kumar 1998a, Suresh Kumar 1998b). Full-scale study on pressure equalization of rainscreen facades is the subject of this paper.

Most of the previous full-scale studies reported only the performance of the rainscreen cladding of the existing buildings (Suresh Kumar 1998a); the measurements carried out by Ganguli and Dalgliesh (1988) and Straube (1998) are noteworthy. On the other hand, it is worthwhile to carry out a full-scale study where the parameters such as cavity volume, leakage area, venting area can be varied. This paper reports such a systematic field investigation concerning pressure equalization performance of rainscreen facades carried out at TUE in the Netherlands. The field facility and the measurement results are presented. In particular, this paper focuses on analysis of the field data in the frequency domain. Further, a first attempt to synthesize the experimental results towards codification is also presented. A few preliminary results of this study were reported in Suresh Kumar and Wisse (1999).

2. Experimental procedure

2.1. Test site

The experiments have been performed on the main building of TUE, Eindhoven. The dimensions of this building are length = 167 m, width = 20 m and height = 44.6 m. This building has an exact north-south orientation so that the long facades are facing west and east directions. Prevailing strong wind directions are west and southwest. The terrain condition on prevailing wind directions is suburban. Further details on test site can be found elsewhere (Geurts 1997).

2.2. Meteorological tower and test panel

The SOLENT ultrasonic anemometer (for features - see Suresh Kumar 1999) mounted at the top of 30 m high mast placed on a 14 m high building, 127 m westward of the main building of the university was used for three component wind velocity measurements. The facade of the main building is a curtain wall made of glass windows and steel parapets on steel columns; the distance between the steel columns is 1.24 m center to center. For this investigation, the glass cladding of a facade-element was replaced with a test panel. This wooden panel of size 1 m $\times$ 1.3 m (panel area, $A_w = 1.3\ \mathrm{m}^2$) was mounted approximately on the middle of the west facade at a height of about 39 m above the ground. The field facility is pictorially shown in Fig. 1.

The test panel consists of three components: (1) rainscreen, (2) air barrier and (3) an air space (cavity) between them; the cavity depth can be varied. Four pressure taps each were installed on the rainscreen and air barrier for pressure measurements. Fig. 2 shows the details of the used test panel. Two venting area types were used: (1) sharp-edged circular holes of 3 mm diameter and 0.5 mm depth (see Fig. 2), and (2) two rectangular slits of dimensions length = 200 mm, width = 11.5 mm, depth = 20 mm (see Fig. 3). Venting area can be varied by closing the holes. Also, two air barrier leakage types were used: (1) three sets of straws, each 15 cm long and 5 mm dia., in three circular holes (dia. 2 cm, 3.8 cm, 2 cm) at three different locations in the middle of the panel, and (2) industrial metal filter. Fig. 4 shows the sketch of the air barrier leakage configurations. Pressure and velocity data were collected for six panel configurations. Table 1 presents the details of these configurations. The flow characteristics of venting and air barrier leakage reported in Table 1 were determined using simple static pressurization tests; details of these tests are provided in Suresh

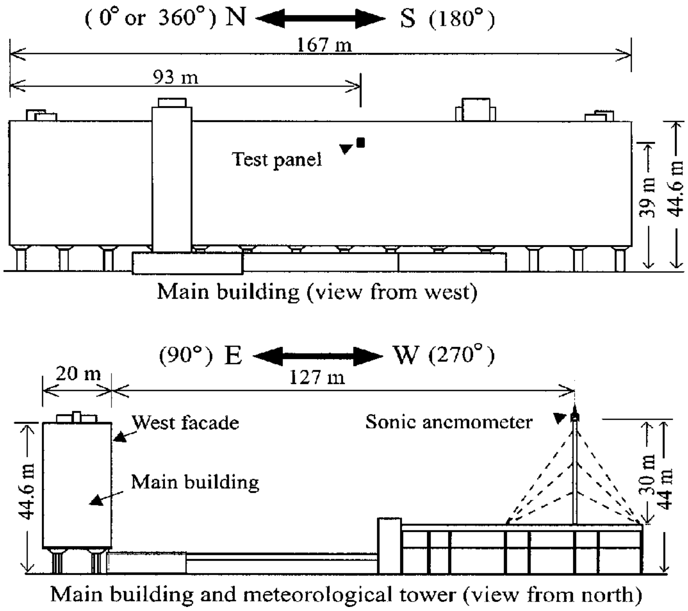

Fig. 1 Sketch of the field facility

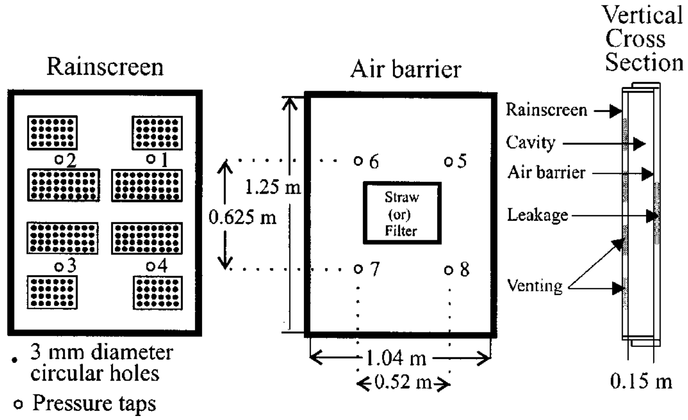

Fig. 2 The test panel

Kumar (1999). For all these configurations, the cavity depth was kept constant at 0.15 m. Note that configurations 1 and 2 are different only in venting area; the venting area of configuration 1 ($A_{rs1} \approx 0.0075A_w$) is about 5 times higher than the venting area of configuration 2 ($A_{rs2} \approx 0.0015A_w$). For configuration 1, the venting area is approximately 6 times the leakage area, while for configuration 2, the leakage area is as high as the venting area. Comparing configurations 2 and 3, the venting areas are same; however, their leakage characteristics are quite different. Configurations 4 and 5 have airtight air barrier (i.e., no leakage), but their venting geometry's are different; the venting area of configuration 5 is about 2.3 times the venting area of configuration 4. Configuration 6 is the same as configuration 5 but with leaky air barrier. Using simple mass balance equation connecting airflow into the cavity with the airflow out of the cavity (Suresh Kumar and van Schijndel 1998, Suresh

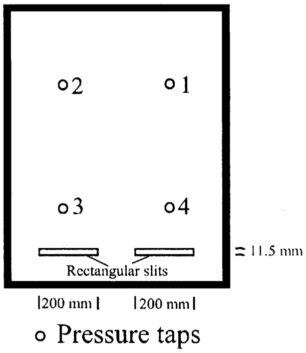

Fig. 3 Rainscreen with rectangular slits

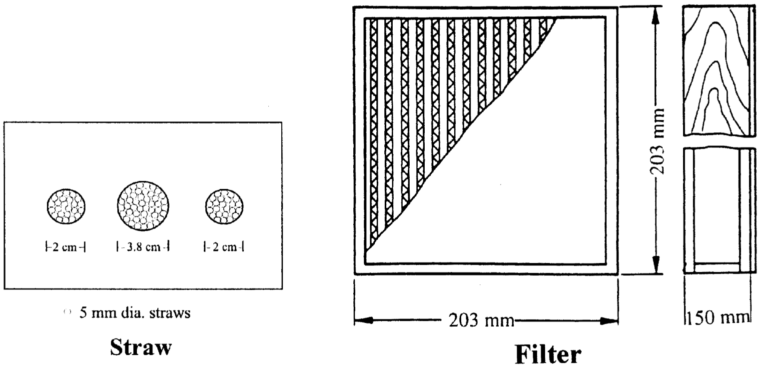

Fig. 4 Air barrier leakage configurations

Table 1 Panel configurations used for field measurements

Configuration	**1**	**2**	**3**
Venting	Circular holes A_{rs} = 0.009613 C_d = 0.61, $n1$ = 0.5	Circular holes A_{rs} = 0.001979 C_d = 0.61, $n1$ = 0.5	Circular holes A_{rs} = 0.001979 C_d = 0.61, $n1$ = 0.5
Air barrier leakage	Straw C_{ab} = 0.000314 $n2$ = 0.71	Straw C_{ab} = 0.000314 $n2$ = 0.71	Filter C_{ab} = 0.000171 $n2$ = 1.0
Configuration	**4**	**5**	**6**
Venting	Circular holes A_{rs} = 0.001979 C_d = 0.61, $n1$ = 0.5	Rectangular slits A_{rs} = 0.004577 C_d = 0.61, $n1$ = 0.5	Rectangular slits A_{rs} = 0.004577 C_d = 0.61, $n1$ = 0.5
Air barrier leakage	No leakage	No leakage	Filter C_{ab} = 0.000171 $n2$ = 1.0

Note: A_{rs} = venting area (m^2), C_d = discharge coefficient, $n1$ = flow exponent of air barrier, C_{ab} = flow coefficient of air barrier (mPa^{-n2}/s), $n2$ = flow exponent of air barrier.

Kumar and van Schijndel 1999), it can be easily shown that configurations 1, 4 and 5 are more effective than the other configurations 2, 3 and 6 in equalizing cavity pressure with the external pressure. The order of preference of these configurations is 5, 4, 1, 6, 2 and 3.

2.3. Instrumentation

Differential pressure transducers supplied by Micro Switch were used to measure the differential pressures across the panel and across the air barrier, i.e., the difference between the external or cavity pressure and a reference pressure, preferably the ambient pressure. Pressure transducers tend to drift in time. In addition to this, full-scale measurements are usually done over long periods of time and data acquisition is done automatically. Therefore, special precaution was taken in these measurements to arrest the drift of the pressure transducers using voltage regulators. The calibration of the pressure transducers is reported in Suresh Kumar (1999).

Pressure transducers were placed behind the surface, connected by flexible tubing to pressure taps on the surface. It is reported in literature that too long and narrow tubes can cause attenuation of the fluctuating pressures and filter high frequencies of interest. In this study, tubes of internal dia. 6 mm and length 0.5 m were used to connect the pressure taps with the Micro Switch transducers; the frequency response of this tubing system is flat at least up to 20 Hz (Geurts 1997).

The choice of reference pressure can have a large influence on the measured differential pressures. For buildings in a built-up area and for high-rise buildings, an undisturbed measurement of ambient reference pressure is practically impossible (Geurts 1997). Though internal pressure can be used as the reference pressure, corrections on the measured pressures are needed due to the deviation of internal pressure from ambient pressure; this issue is discussed in Suresh Kumar (1999). In this study, internal building pressure is used as the reference pressure. To avoid any abrupt internal pressure variations, tubes of dia. 4 mm connected at the reference edge of the transducer were put in a thermally insulated flask placed in a protected location.

For data acquisition, a Physics Data Acquisition System (PhyDAS) developed at the Faculty of Physics of the TUE was used. A PARSAM 25 (Parallel sampling A/D conversion board) was used to capture the incoming signal. PARSAM can read 16 analogue signals simultaneously and convert into digital values. The instrumentation features are provided in Suresh Kumar (1999).

2.4. Data collection

In each run, the exterior and cavity pressure data were simultaneously measured at four taps each at a sampling rate of 20 Hz for 10 minutes. The velocity data were also acquired by PhyDAS at a rate of 20.83 Hz. The data were written automatically to the hard disk of a personal computer. Analysis of the data was carried out using UNIX workstation. The data acquisition was controlled by the mean wind velocity measurements; the data acquisition is set to trigger when the mean wind velocity in the last minute exceeds a preset value of 6 m/s. The measurements were carried out between May 1998 and July 1999. During this period, each of the six configurations was set for at least about two months each for measurements. About 1500 full-scale runs were registered.

2.5. Data analysis

Firstly, representative differential pressure time series across the panel (P) and across the air barrier (P_{ab}) were calculated by respectively averaging the measurements at four exterior taps (1, 2, 3 & 4 - see Fig. 2) and at four cavity taps (5, 6, 7 & 8 - see Fig. 2). Thereafter, the collected data were screened in order to simplify analysis as well as to obtain meaningful results. Pressure records that are stationary (Geurts 1997) and measured during which the turbulent intensity is less than 0.35, the mean horizontal wind speed is greater than 6 m/s, the mean wind direction is between 180^o and 360^o (see Fig. 1), and the root-mean-square (rms) wind direction is less than 20^o were selected for further analysis. These current measurements concentrate only on the performance of the panels to wind conditions favoring rain penetration (i.e., positive wind pressures). However, for meaningful wind design of rainscreen, measurements are needed in separation zones where largest suction pressures occur, though these outward pressures are not threatening rain penetration. Restriction over rms wind direction was made in order to draw meaningful comparison of pressures over different wind directions. All the six configurations together, about 1200 records were selected for further analysis. The selected records were analyzed in time, frequency and amplitude domains. Representative samples of field data have been chosen for the demonstration of the results reported mainly in the frequency domain. Finally, pressure values were converted to non-dimensionalized pressure coefficients using the dynamic pressure at panel height.

3. Experimental results

Sample measured wind direction, wind velocity and pressure time histories are shown in Fig. 5 for configuration 2. The estimated differential pressure across the rainscreen or rainscreen pressure ($P_{rs} = P - P_{ab}$) is also shown. Note that the differential pressures across the air barrier (P_{ab}) are smoother than those across the panel (P). This shows that the higher frequency differential pressures across the panel are attenuated in the cavity, signifying that the higher frequency differential pressures across the panel are transmitted to the rainscreen. To illustrate these points clearly, the spectral density functions ($S(f)$) of pressure time histories normalized by corresponding variances (σ^2) are shown in Fig. 6. As expected, the amplitudes of the spectrum of the differential pressure across rainscreen at higher frequencies are much higher than those of the spectrum of P and P_{ab}. The statistics of the pressure time series corresponding to Fig. 5 are provided in Table 2. For this particular case, the rainscreen carries approximately 38% of the total mean load across the panel as well as the rms load across the panel, and 43% of the absolute maximum load across the panel.

An interesting frequency domain method of analysis, estimation of transfer function has been carried out in order to relate the input (differential pressure across the panel, P) and the output (differential pressure across the rainscreen, P_{rs} or differential pressure across the air barrier, P_{ab}) of a PER facade system (Suresh Kumar and Wisse 1999). The transfer function for the differential pressure across the air barrier (magnitude, $|H_{ab}(f)|$ and phase lag, $\phi_{ab}(f)$) is shown in Fig. 7. The magnitude of the transfer function is a measure of the ratio of wind pressures equalized as a function of frequency; value 1 indicates full pressure equalization occurred, i.e., no pressure acting on the rainscreen and maximum pressure acting on the air barrier. Mean exterior pressure experiences an attenuation of 38% (see Table 2); the low frequency exterior pressures also experience similar attenuation as shown in Fig. 7. The magnitude of the transfer function (i.e., pressure equalization ratios) drops rapidly only after about 3 Hz; rapid shift in phase lag is also observed after about 3 Hz. This once again confirms the poor performance of this configuration to equalize higher frequency pressure fluctuations. Note that higher pressure equalization ratios at lower frequencies can be obtained by increasing the venting area. The pressure equalization performance can also be presented using the transfer function for the differential pressure across the rainscreen. The magnitude of this transfer function ($|H_{rs}(f)|$) is a measure of the ratio of wind pressures acting on rainscreen as a

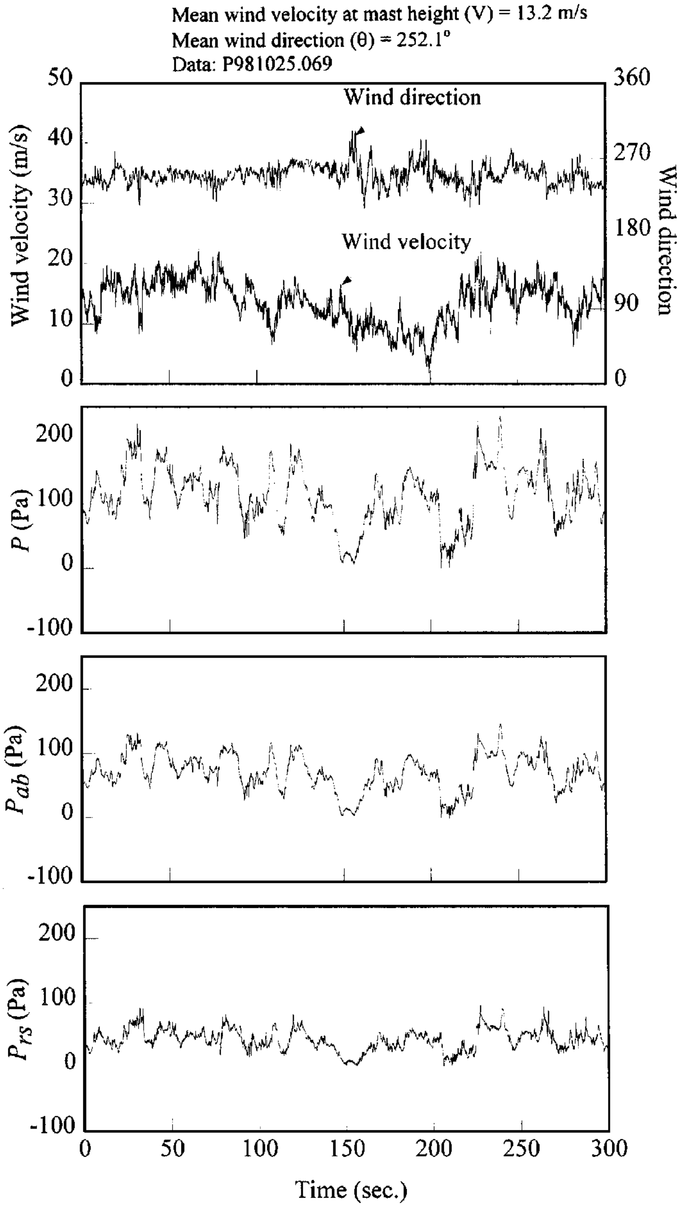

Fig. 5 Measured time histories (configuration 2)

function of frequency; value zero indicates no pressure acting on rainscreen, i.e., full pressure equalization occurred. A typical example is shown in Fig. 8; the observations are similar to those noticed in Fig. 7 but in an alternative form.

The probability density functions of the pressure fluctuations are shown in Fig. 9. The shift in mean pressures is clear. Moreover, the differential pressure across the rainscreen is somewhat positively skewed. The rainscreen acts as a filter, decreasing the range of pressure fluctuations acting on it. This filtering effect is different for different configurations. In case of configuration 1, a

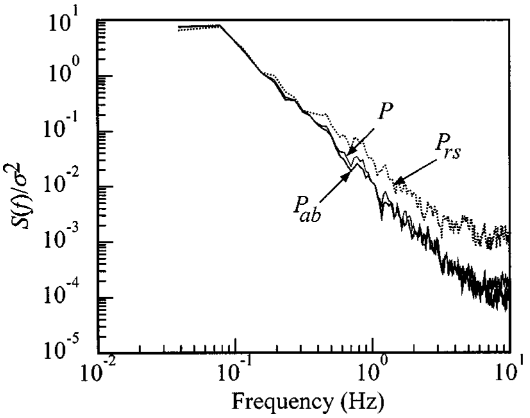

Fig. 6 Spectral density functions (case - Fig. 5)

Table 2 Statistics of pressures (case - Fig. 5)

	P (Pa)	P_{ab} (Pa)	P_{rs} (Pa)
mean	100.5	62.5	38.0
rms	42.6	27.1	16.0
abs(max)	234.9	146.3	101.6

Note: abs(max) = absolute maximum

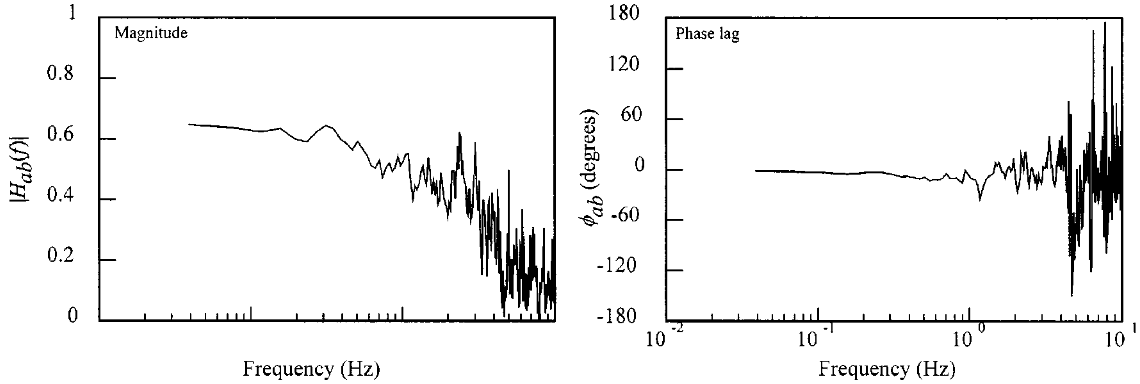

Fig. 7 Transfer function for the differential pressure across the air barrier (case - Fig. 5)

pronounced filtering has been noted because of its larger venting area.

Pressure attenuation in the cavity is mainly caused by spatial pressure variations and damping of flow through the vents and in the cavity. The coherence between differential pressures across the panel at two exterior taps and between differential pressures across the air barrier at two corresponding cavity taps is shown in Fig. 10. The coherence between differential pressures across the panel drops rapidly for frequencies above 0.5 Hz. On the other hand, the coherence between differential pressures across the air barrier at these two locations drops rapidly only after about 3 Hz. This is the result of an averaging effect of pressures over a compartment for frequencies between 0.5 Hz and 3 Hz. The effects of damping can be identified at 3 Hz, where damping started to disturb the

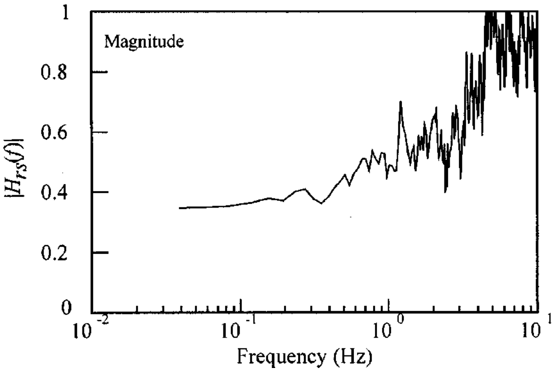

Fig. 8 Transfer function for the differential pressure across the rainscreen (case - Fig. 5)

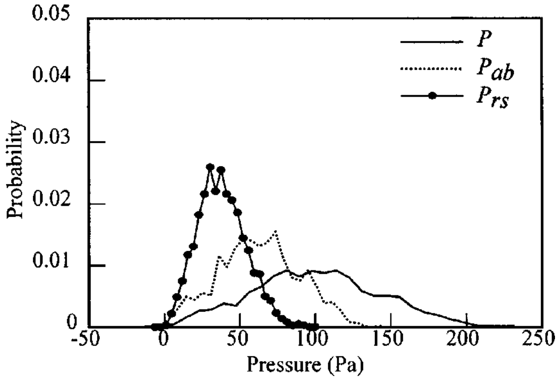

Fig. 9 Probability density function (case - Fig. 5)

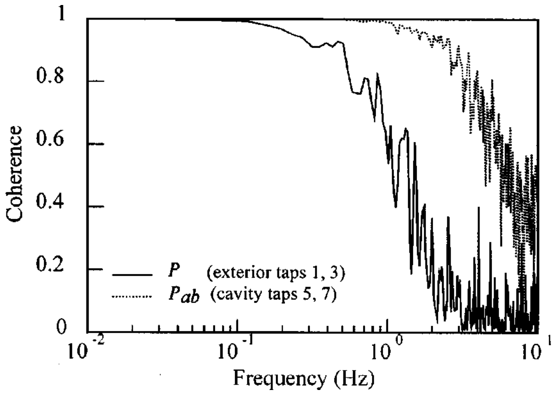

Fig. 10 Coherence between differential pressures across the panel and between differential pressures across the air barrier (case - Fig. 5)

equalization process causing a non-uniform pressure across the compartment. Facade characteristics are mainly responsible for the pressure attenuation in the cavity at low frequencies. It is also observed from the time series plots that the pressure variations across the air barrier are closely following the pressure variations across the panel without noticeable time lag; this is due to the fast response of the wall system under consideration. In almost all cases, the correlation between P and P_{ab} is found to be 99%.

3.1. Influence of venting area

Venting area significantly affects the pressure equalization performance of the panel. For demonstration, time series data corresponding to the same wind velocity and direction, from two configurations with the only difference in venting area, are considered. Typical examples are shown in Fig. 11. Note that configuration 2 with a venting area of $0.0015A_w$ transfers 30% of low frequency wind pressure fluctuations to the rainscreen (i.e., 70% pressure equalization), while configuration 1 with a venting area of $0.0075A_w$ transfers only about 3% of low frequency wind pressure changes to the

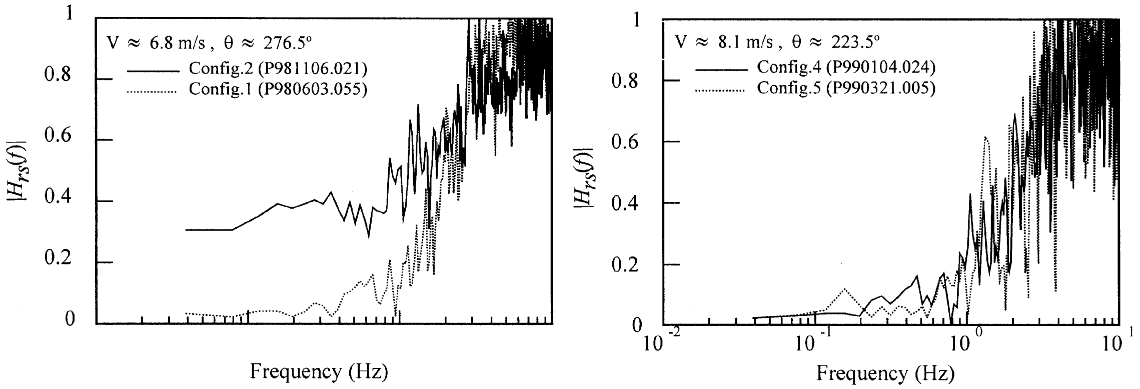

Fig. 11 Influence of venting area

rainscreen (i.e., 97% pressure equalization). Pressure equalization performance of configuration 1 with higher venting area is appreciably higher at least up to 2 Hz compared with the case of configuration 2. However, high frequency wind pressure fluctuations are transferred to the rainscreen almost at the same rate in both cases.

Fig. 11 also compares the influence of venting area in case of configurations 4 and 5 having airtight air barrier. Note that configuration 4 with a venting area of $0.0015A_w$ and configuration 5 with a venting area of $0.0035A_w$ transfer almost the same amount of low as well as high frequency fluctuations to the rainscreen. Note the similarity of these curves with that of configuration 1. As expected, in case of configuration 1 having leaky air barrier, the panel needs larger venting area to achieve better pressure equalization performance compared to configurations 4 and 5 having airtight air barrier. On the other hand, in case with airtight air barrier, smaller venting area may be sufficient to achieve better pressure equalization performance; the transfer function magnitudes of configuration 5 are almost the same as those of configuration 4, though the venting area of configuration 5 is about 2.3 times the venting area of configuration 4. It is revealed that the difference in transfer function magnitudes at low frequency region of configurations 2 and 4 is primarily due to the leakage characteristics of the air barrier used.

Overall, the pressure equalization performance of the panel is greatly influenced by the amount of venting provided. The influence of venting area is predominant especially when the air barrier is leaky. Small amount of venting area is enough to provide reasonable pressure equalization when the air barrier is airtight. Influence of venting is found to be only in the low frequency region; the pressure equalization performance seems indifferent in the high frequency region irrespective of the different venting characteristics.

3.2. Influence of air barrier leakage

The influence of air barrier leakage is similar to that of venting area. For demonstration, time series data corresponding to the same wind velocity and direction, from two configurations with the only difference in leakage characteristics, are considered. Fig. 12 shows the performance of the panel with different air barrier leakage configurations. Note that air barrier leakage of configuration 3 is higher than that of configuration 2. This results in transferring major part of the low as well as the high frequency fluctuations to the rainscreen in case of configuration 3. Note the similarity

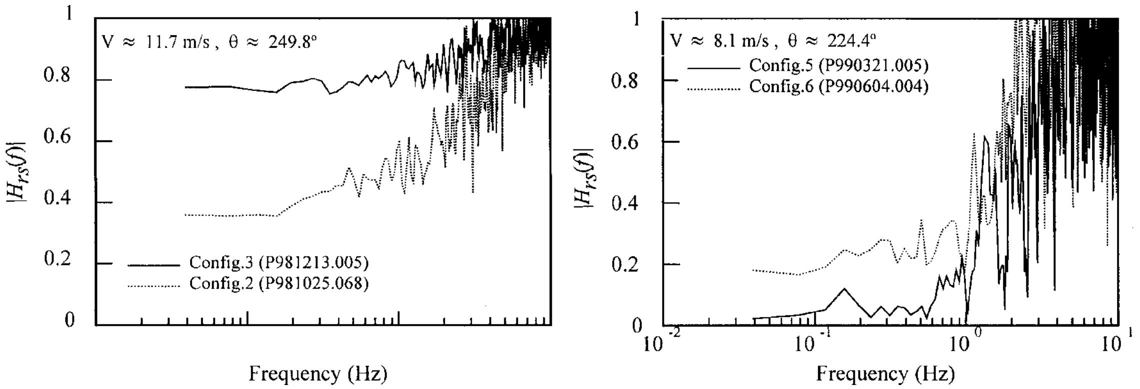

Fig. 12 Influence of air barrier leakage

between the transfer functions of the configuration 2 shown in Figs. 11 and 12 though they correspond to different wind velocities and directions. In the same figure, configuration 6 with air barrier leakage and configuration 5 without leakage are considered for comparison. As expected, configuration 6 transfers higher percentage of low frequency wind pressures to the rainscreen due to its leaky air barrier.

3.3. Influence of wind velocity

It is found in this study that the influence of wind velocity on pressure equalization is predominant in case of leaky air barrier configurations. For demonstration, time series data corresponding to the same wind direction but different wind velocities, for specific configurations are considered. Typical examples are shown in Fig. 13. In case of configuration 3, smaller percentage of long duration wind pressures is transferred to the rainscreen at lower wind velocities. This is presumably due to the large difference in flow exponents between the rainscreen and air barrier, as shown in Table 1, causing high dependency of rainscreen pressures on differential pressures across the panel (Inculet 1990, Suresh Kumar 1998a). Higher differential pressures across the panel caused by high wind velocity induce higher rainscreen pressures resulting in higher percentage of load sharing by the rainscreen and correspondingly, higher transfer function magnitudes. In the event of low wind velocity, the corresponding lower differential pressures across the panel induce lower rainscreen pressures resulting in lower percentage of load sharing by the rainscreen and correspondingly, lower transfer function magnitudes. However, noticeable influence of wind velocity on pressure equalization is almost rare in case of configuration 2; this is due to the comparatively small difference in flow exponents between the rainscreen and air barrier. In case of configuration 1, the transfer function amplitudes corresponding to different velocities are indistinguishable as shown in Fig. 13. This indicates that the influence of wind velocity can be reduced by providing larger venting area even when the flow through the air barrier is laminar (n_2 = 1). In case of configuration 5 with no leakage, the transfer function amplitudes corresponding to different velocities are almost the same. Overall, Figs. 11, 12 and 13 indicate that providing an airtight air barrier may be a wise solution to achieve better pressure equalization performance of the panel.

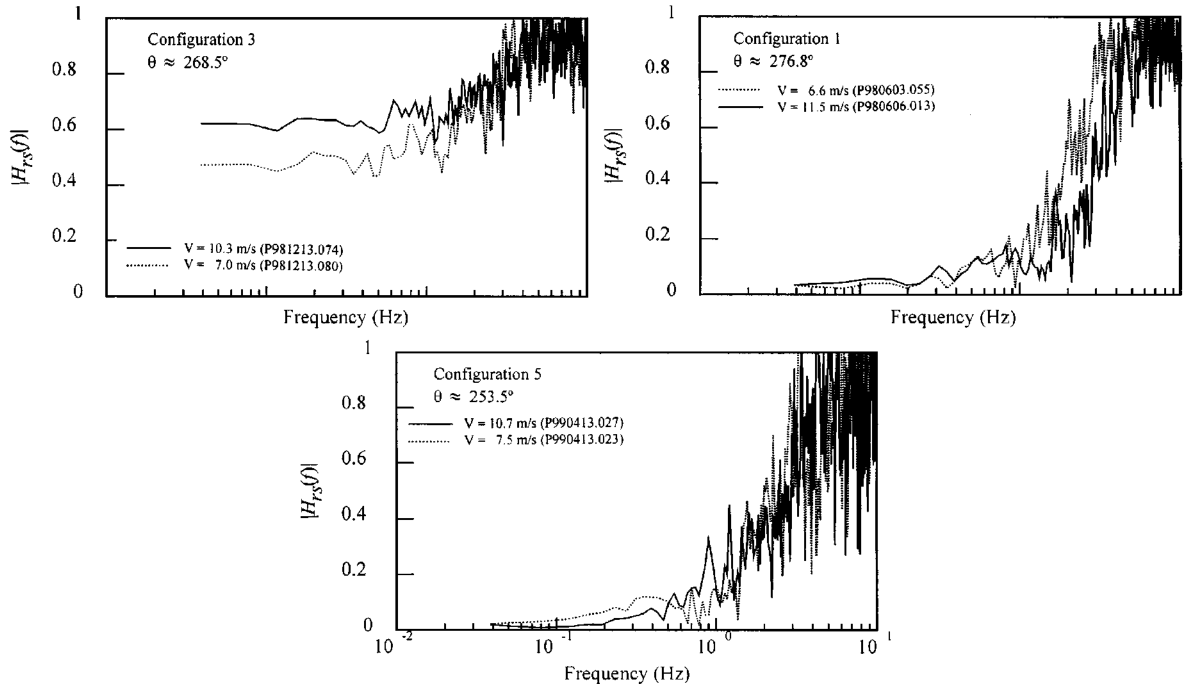

Fig. 13 Influence of wind velocity

3.4. Influence of wind direction and panel location

Analysis showed that wind direction do have an influence on the pressure equalization performance of the panel. For demonstration, time series data corresponding to the same wind velocity but different wind directions, for specific configurations are considered. Typical examples are shown in Fig. 14. The influence of wind velocity is once again clear in case of configuration 3 with leaky air barrier and reduced venting area; the curves corresponding to $V = 9$ m/s are higher than the curves corresponding to $V = 5.2$ m/s. However, such a rise in the transfer function magnitudes corresponding to the rise in the wind velocities is not observed in case of configuration 6 though this has the same air barrier leakage as of configuration 3; this is due to the larger venting area of this configuration. This once again shows that the adverse effect of air barrier leakage can be surmounted by providing appropriate amount of venting area in order to enhance the pressure equalization performance. Therefore, the leakage characteristics of the air barrier will be a decisive factor towards the provision of the required venting area. The pressure equalization of low frequency pressure fluctuations seems to be dependent on the wind direction, except in the case of no leakage situation (configuration 4) where such dependence is obvious only in the case corresponding to high wind velocity. On the other hand, pressure equalization of high frequency fluctuations is independent of wind direction. In general, higher the angles of wind attack away from the normal to the west facade (270^o), better the pressure equalization of low frequency fluctuations. This is consistent with all the configurations for different wind velocities. Note that the same wind velocity blowing in different wind directions can induce different pressures across the panel. In general, higher the wind attack angle away from the normal to the facade, lesser the pressure induced across the panel and correspondingly, lesser the

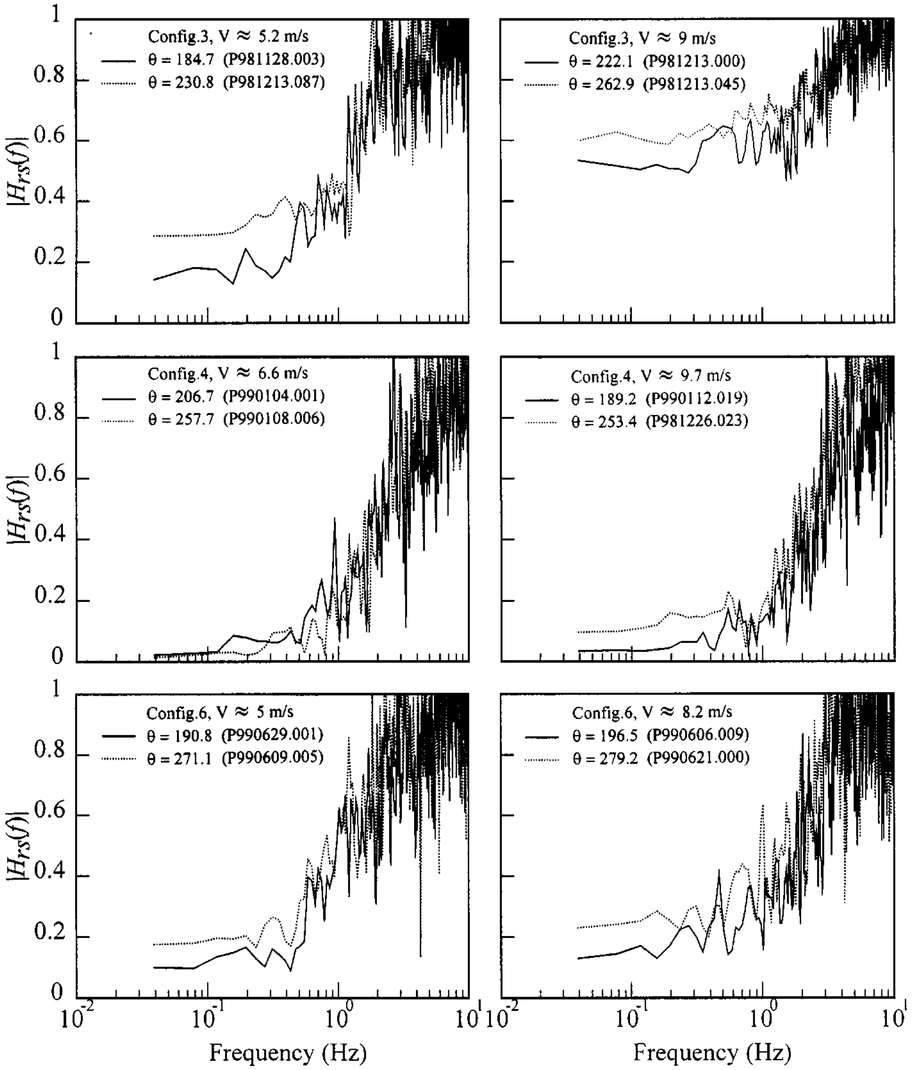

Fig. 14 Influence of wind direction

pressure induced across the rainscreen. As previously noted, the load sharing by the rainscreen depends on the total pressure drop across the panel due to the difference in flow exponents between the rainscreen and air barrier. As a result, when the wind attack angle deviates away from normal to the facade, the percentage of load sharing by the rainscreen and correspondingly, the transfer function magnitudes reduce.

Poor pressure equalization performance is expected when the panel is subjected to wind loading which contains more high-frequency/short duration gusts. In this study, panel is located near the middle of the building. It is found that this panel did not experience high spatial pressure variations because of its smaller size and location. It is very likely that the panels located on edges and corners may undergo high spatial pressure variations; these panels have to be more or less the same size of this panel to achieve acceptable performance.

4. Towards codification

Quantification of the wind-induced differential pressure across the rainscreen with respect to that across the panel is needed for developing design guidelines for rain penetration control as well as structural load reduction. Towards this goal, a methodology quantifying the rainscreen load in terms of the panel load has been proposed. This methodology represents the peak differential pressure across the rainscreen as a function of the mean, rms and peak factor of the differential pressure across the panel using three coefficients. The values of these coefficients based on field measurements are also provided.

Based on the assumption of rigid rainscreen walls under spatially uniform wind pressures, the expression used in the Dutch code (NEN 6702 1991) for the estimation of representative wind-induced differential pressure (P_{rep}) across the rainscreen of a pressure equalized rainscreen facade can be reduced to

$$P_{rep} = C_{eq} \cdot (\bar{P} + g_p\tilde{P}) = C_{eq} \cdot \hat{P} \tag{1}$$

where, the coefficient C_{eq} accounts for pressure equalization, $\bar{P}$, $\tilde{P}$, $\hat{P}$ and g_p are respectively the mean, rms, peak and peak factor of the differential pressure across the panel. The current code suggested a value of one for C_{eq} until pertinent information becomes available. Note that the term inside the parenthesis of Eq. (1) represents the peak differential pressure across the panel ($\hat{P}$) and this is the representative differential pressure across the rainscreen if there is no pressure equalization involved, i.e., $C_{eq} = 1$. If the panel is pressure equalized to some degree, then intuitively, C_{eq} is the ratio of the peak differential pressure across the rainscreen ($\hat{P}_{rs}$) to the peak differential pressure across the panel ($\hat{P}$). By this definition, $C_{eq} = 1$ indicates no pressure equalization occurred, i.e., full pressure acting on the rainscreen, and $C_{eq} = 0$ indicates full pressure equalization occurred, i.e., no pressure acting on the rainscreen. However, it is found in this investigation that this ratio cannot be quantified easily because this somehow addresses both the so called static as well as dynamic pressure equalization processes. In order to simplify this problem, static pressure equalization coefficient (C_{eqs}) and dynamic pressure equalization coefficient (C_{eqd}) are introduced instead of a single C_{eq}.

Eq. (1) is rewritten as

$$P_{rep} = \hat{P}_{rs} = C_{eqs}.\bar{P} + C_{eqd}.g_p\tilde{P} \tag{2}$$

where,

$$C_{eqs} = \frac{\bar{P}_{rs}}{\bar{P}} \tag{3}$$

$$C_{eqd} = C_s.C_g \tag{4}$$

where,

$$C_s = \frac{\tilde{P}_{rs}}{\tilde{P}} = \frac{\sqrt{\int_0^\infty S_{rs}(f)df}}{\sqrt{\int_0^\infty S_p(f)df}} \tag{5}$$

$$C_g = \frac{g_{rs}}{g_p} \tag{6}$$

where, $\bar{P}_{rs}$, $\tilde{P}_{rs}$, $S_{rs}(f)$ and g_{rs} are respectively the mean, rms, spectrum and peak factor of rainscreen pressures, and $S_p(f)$ is the spectrum of differential pressure across the panel. Substituting Eqs. (3) - (6) in Eq. (2) yields:

$$\hat{P}_{rs} = \bar{P}_{rs} + g_{rs}\tilde{P}_{rs} \tag{7}$$

The values of the coefficients C_{eqs}, C_s and C_g are required for the estimation of the peak pressure acting on the rainscreen. It appears from this investigation that the quantification of C_s may be difficult compared to C_{eqs} and C_g. By introducing the screen admittance function, $|H_{rs}(f)|^2$ (i.e., square of the magnitude of the transfer function for rainscreen pressures), $S_{rs}(f)$ can be evaluated from $S_p(f)$ using,

$$S_{rs}(f) = |H_{rs}(f)|^2 S_p(f) \tag{8}$$

Substituting Eq. (8) in Eq. (5) yields:

$$C_s = \frac{\sqrt{\int_0^\infty |H_{rs}(f)|^2 S_p(f)\,df}}{\sqrt{\int_0^\infty S_p(f)\,df}} \tag{9}$$

Note that spatial variation of pressures over a panel can influence the screen admittance function as well as the spectrum of pressures across the panel. Therefore, the coherence of pressure fluctuations on a panel should be considered while developing an expression for these quantities; this has to be investigated further.

Fig. 15 shows the measured C_{eqs} values with respect to the corresponding mean pressure coefficients for the panel. C_{eqs} is the ratio of mean rainscreen pressure to the mean panel pressure; higher C_{eqs} values indicate poor pressure equalization and higher mean load sharing by the rainscreen. Note that C_{eqs} values increase as the mean pressure coefficients decrease for all the configurations. For a particular configuration, C_{eqs} values more or less stabilize to lower values for higher absolute mean pressure coefficients. Since higher mean pressure coefficients across the panel induce higher mean rainscreen pressures, the corresponding lower C_{eqs} values may be of interest for design. Note also that these stabilized C_{eqs} values are different for each configuration. As expected, configurations 2 and 3 have higher C_{eqs} values compared to all other configurations.

Fig. 16 shows the measured C_s values with respect to the corresponding rms rainscreen pressure coefficients. C_s is the ratio of rms rainscreen pressure to the rms panel pressure; higher C_s values indicate poor pressure equalization and higher rms load sharing by the rainscreen. It is clear that low C_s values are associated with low rms rainscreen pressure coefficients. In case of configurations 2 and 3 with leaky air barrier and smaller venting area, the measured rms rainscreen pressures are high corresponding to the high rms panel pressures. Consequently, the C_s values are high in both configurations. On the other hand, in case of other configurations, the rms rainscreen loads are low

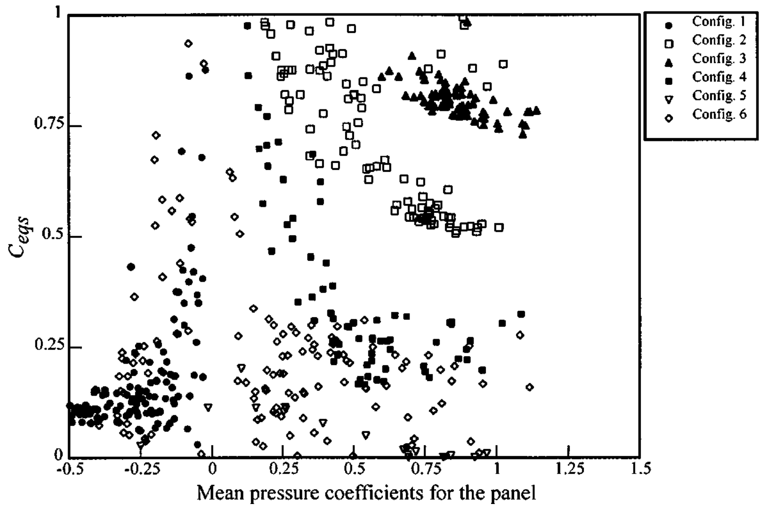

Fig. 15 Measured values of C_{eqs}

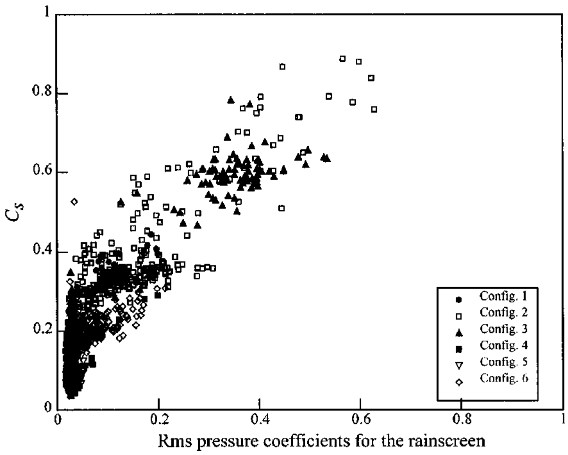

Fig. 16 Measured values of C_s

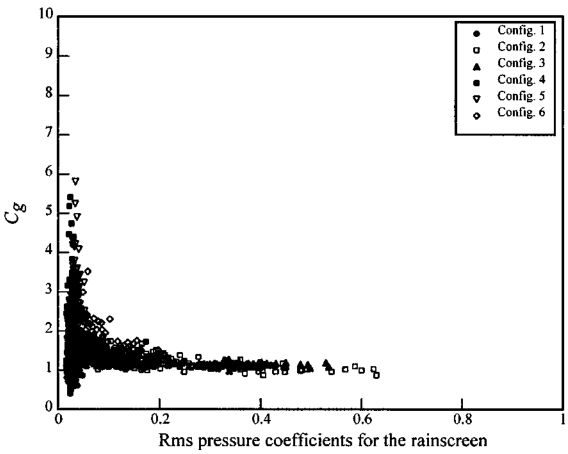

Fig. 17 Measured values of C_g

and the associated C_s values are low. This shows that lower C_s values can be achieved by providing adequate venting area for counteracting the leakage of the air barrier.

Fig. 17 shows the measured C_g values with respect to the corresponding rms rainscreen pressure coefficients. C_g, a ratio of peak factor of rainscreen pressure to the peak factor of panel pressure, is computed using the maximum pressures acting on the panel and rainscreen. Note that the values of C_g are generally greater than one. This shows that the peak factors for rainscreen pressures are, in general, higher than those for pressures across the panel. Very high C_g values typically occur for low rms pressure drops across the rainscreen; this seems to be an overestimation of the values. Since the high rms rainscreen pressures are of interest for design, C_g values associated with high rms rainscreen pressures should be carefully investigated. Based on the measurement results, C_g value of 2 seems appropriate for design. The suggested C_g value of 3 by Inculet (1990) seems to be on the higher side. Note that even lower C_g values can be obtained by considering proper averaging time (typically 1 second is used for cladding design) for the peak selection.

5. Conclusions

Extensive full-scale measurements of wind velocity and wind-induced pressures across the panel and rainscreen were carried out at TUE in the Netherlands. During this period, six panel configurations with different venting area, venting location, venting geometry and air barrier leakage characteristics were tested. It is noted that the pressure experienced by the rainscreen increases as the differential pressure across the panel increases when the airflow through the air barrier approaches laminar flow. Pressure equalization of mean as well as low frequency pressures can be achieved by providing adequate venting area with respect to the area of the panel and leakage characteristics of the air barrier. On the other hand, pressure equalization of the short duration pressure fluctuations seems hardly possible. All configurations exhibit very little pressure equalization of high frequency wind gusts; the characteristics of wind have predominant influence on the maximum achievable degree of pressure equalization at higher frequencies. On the other hand, facade characteristics do have an effect on the degree of pressure equalization, especially at lower frequencies. This is the first time, detailed full-scale results in the form of transfer functions and pressure coefficients are utilized to comprehend the influence of various parameters on pressure equalization performance.

Towards the quantification of peak load acting on the rainscreen, static and dynamic pressure equalization coefficients have been formulated; the variation of the measured values of these coefficients is discussed. The influence of facade and wind characteristics on the values of these coefficients should be investigated further.

In summary, through extensive full-scale measurements, this research work acquired comprehensive knowledge about the influence of wind as well as facade parameters on pressure equalization performance of rainscreen facades. However, more measurements on different panel configurations and on panels located in separation zones are needed to collect the volume of data required to set the design guidelines.

Acknowledgements

Financial support for this project provided by the Netherlands School for Advanced Studies in Construction is gratefully acknowledged. The authors would also like to thank Mr. Eric Wijen and Mr. Wim van de Ven for their help in setting up the experimental facility.

References

Anderson, J.M. and Gill, J.R. (1988), *Rainscreen cladding: A guide to design principles and practice*, Butterworths, London.

Ganguli, U. and Dalgliesh, W.A. (1988), “Wind pressures on open rain screen walls: Place Air Canada”, *J. Struct. Eng.*, ASCE, **114**(3), 642-656.

Geurts, C.P.W. (1997), “Wind-induced pressure fluctuations on building facades”, Ph.D. Thesis, Faculteit Bouwkunde, Technical University of Eindhoven, the Netherlands.

Inculet, D.R. (1990), “Pressure-equalization of rainscreen cladding”, M.E.Sc. Thesis, The University of Western Ontario, Canada.

NEN 6702 (1991), *Loadings and deformations TGB 1990*, Technische grondslagen voor bouwconstructies, Nedelands Normalisatie-instituut, the Netherlands.

Straube, J.F. (1998), "Moisture control and enclosure wall systems", Ph.D. Thesis, Civil Engineering Department, University of Waterloo, Canada.

Suresh Kumar, K. (1998a), "Pressure equalized rainscreen approach to wall design: Past accomplishments and future challenges", Technical Report: FAGO 98.25.K, Faculty of Architecture, Building and Planning, Technical University of Eindhoven, the Netherlands.

Suresh Kumar, K. (1998b), "Pressure equalization performance of rainscreen walls: Experimental investigations", *Proc. 2nd East European Conf. Wind Eng.*, Prague, Czech Republic.

Suresh Kumar, K. (1999), *A Study on Pressure Equalization of Rainscreen Facades: Full-scale Experiments and Computer Simulations*, Technical Report, FAGO 99.40.K, Facultiet Bouwkunde, Technical University of Eindhoven, Eindhoven, The Netherlands.

Suresh Kumar, K. (2000), "Pressure equalization of rainscreen walls: A critical review", *Bldg. Envir.*, **35**(2), 161-179.

Suresh Kumar, K. and van Schijndel, A.W.M. (1998), "Cavity pressure dynamics of rainscreen walls", *Proc. 4th UK Conf. Wind Eng.*, Bristol, UK.

Suresh Kumar, K. and van Schijndel, A.W.M. (1999), "Prediction of pressure equalization performance of rainscreen walls", *Wind and Structures*, **2**(4), 325-345.

Suresh Kumar, K. and Wisse, J.A. (1999), "A full-scale study on pressure equalization of rainscreen facades", *Proc. 10th Int. Conf. Wind Eng.*, Copenhagen, Denmark.

C